CHAPTER 51

A SCHEMATIZATION OF ONSHORE-OFFSHORE TRANSPORT

by D.H. Swart*

Abstract

The investigation reported herein covers two aspects of the schematization of coastal processes on sandy beaches in a direction perpendicular to the coastline, viz.: (1) the prediction of equilibrium beach profiles and (2) the corresponding offshore sediment transport due to wave action. A physically-based schematic model of the onshore-offshore profile development was tested on available small-scale and full-scale model tests and physically-based empirical relationships were derived to enable the application of the model to both small-scale and prototype conditions.

1 Analysis

Onshore-offshore transport at any section in a non-equilibrium profile can be characterized as being a combination of bed load transport and suspended load transport. The division between these two modes of transport is not well-defined, due to the complicated water and sediment movement close to the bed. It will, however, be assumed that the total sediment transport in any section can be divided into: (1) bed load, which can be represented as being a sediment concentration multiplied by a layer thickness and a characteristic sediment particle velocity, and (2) suspended load in the form of convection transport in the rest of the section. These assumptions place no restrictions on the further application of the theory.

At the moment the state of the art regarding the prediction of concentration and velocity distribution in the vertical is not so advanced that a uniform theory exists which can predict these two quantities with suitable accuracy both inside the breaker zone and seawards of the breaker point. As it is, however, both in prototype situations and in the design of three-dimensional small-scale models of quite some importance to be able to predict quantitatively the onshore-offshore transport, it was decided to make a schematization of the external properties of the profile development. This external schematization will be used to predict offshore transport until the research regarding the internal mechanism (sediment entrainment, concentration and velocity distribution in the vertical) is so far advanced that onshore-offshore transport can be predicted via the internal mechanisms.

This schematization was aided by all two-dimensional model experiments regarding profile development, available in the Delft Hydraulics Laboratory, as well as by full-scale tests performed by the Coastal Engineering Research Center and supplied to the Delft Hydraulics Laboratory by T. Saville (jr).

* Project engineer, Delft Hydraulics Laboratory, The Netherlands

Consequently the wave conditions of the tests covered o wide ronge, viz.:

$$0{,}07 \text{ m} \leqslant H_o \leqslant 1.71 \text{ m}$$
$$1.04 \text{ s} \leqslant T \leqslant 11.3 \text{ s}$$

The particle diameter showed a smoller voriation, D_{50} voried between 0.1 mm and 0.23 mm, while the bed material in all tests was sand. The waves in all tests were regular waves. As in all Delft Hydroulics Laborotory tests a net seaward movement of sediment occurred, the present paper deals only with the prediction of offshore transport. From the results of the available tests it become apparent that the profile development can be characterized into three definite zones (see Figure 1), each with its own transport mechonism, viz.: (1) the bockshore, which is mostly eroded to above the wave run-up limit, (2) a transition areo at the seaward extremity of the developing profile, which is formed due to the fact thot the point of beginning of movement, londwards of which ripples ond bars ore formed on the bed, does normolly not coincide with the horizontal bed of the flume, and (3) the real developing profile where transport under wave oction takes place (called the D-profile). The some zones also occur in prototype. In order to enable the development of o usoble theory for the prediction of offshore tronsport in the D-profile, it is essential thot the limits between the above-mentioned three areas (zones) can be found uniquely in terms of the wove conditions and bed material characteristics.

2 Limits of the D-profile

From the definition of the bockshore it is opparent that the boundary between the bockshore ond the D-profile, i.e. the upper limit of the D-profile, is o function of the maximum wave run-up.

Using the formula of Hunt [5] for wave run-up, it can be stated in general that the maximum wave run-up η is given by:

$$\eta = a_1 \; H \tan \alpha \left(\frac{H}{\lambda_o} \right)^{b_1} \qquad \ldots\ldots.(1)$$

where H = wove height

$\tan\alpha$ = wetted beach slope

λ_o = deep water wove length

a_1 and b_1 = constants

Wiegel [10] determined the relationship between the beach slope and the median particle diameter D_{50}. For all types of beaches he found a general relationship of the form:

$$\tan a = a_2 \, D_{50}^{\,c_2} \qquad \ldots\ldots.(2)$$

where a_2 and c_2 = constants, depending on the type of beach under consideration;
$c_2 > 0$.

Combination of equations (1) and (2) and regrouping of the terms yielded a general equation for the dimensionless upper limit of the D-profile of the following form:

$$\frac{h_o}{D_{50}} = f(H_o^{\,e} \, D_{50}^{\,c} \, T^b) \qquad \ldots\ldots.(3)$$

where h_o = upper limit of D-profile relative to the still-water level. When all the available small-scale and full-scale data were correlated to equation (3), the following relationship was found (see Figure 2):

$$\frac{h_o}{D_{50}} = 7644 - 7706 \exp\left(-\,0.000143 \; \frac{H_o^{\,0.488} \, T^{\,0.93}}{D_{50}^{\,0.786}}\right) \qquad \ldots\ldots.(4)$$

The lower limit of the D-profile does not coincide with the point of beginning of movement, as predicted by for instance Goddet [4] and Bonnefille and Pernecker [1] , but is assumed to be some function of it. Physically it can be seen as a transition between the area of combined bed load and suspended load (the D-profile) and only bed load (transition area). Analogous to the above-mentioned studies [1], [4] regarding beginning of movement of sediment under wave action, it will thus be assumed that:

$$\frac{h_m}{\lambda_o} = f\left(\frac{H_o^{\,a}}{T^b D_{50}^{\,c}}\right) \qquad \ldots\ldots.(5)$$

where h_m = lower limit of the D-profile, relative to the still-water level
a,b and c = constants as long as $D_{50} \leqslant 0.5$ mm (see [1]).

Correlation of equation (5) to the available small- and full-scale data led to a relationship for the lower limit of the D-profile of the following form (see Figure 3):

$$\frac{h_m}{\lambda_o} = 0.0063 \exp\left(4.347 \; \frac{H_o^{\,0.473}}{T^{0.894} D_{50}^{\,0.093}}\right) \qquad \ldots\ldots.(6)$$

3 Transport schemotizotion in the D-profile

In order to be oble to formulote o simplified form for the transport formulo, it is essentiol to make one ossumption, viz. that the developing beach will eventuolly reach o stoble situotion under persistent wove action. This stable situation implies two aspects, viz. (1) an equilibrium position ond (2) an equilibrium form of the profile. As can be seen from Figure 4, in which a measure of the volume of sediment in the D-profile relative to the point of maximum wave run-up, (L_2-L_e), has been plotted ogainst time for o small-scale test which lasted in total 3878 hours, the concept of equilibrium is a reasonable one. Using this assumption it is possible to write up an equation for the determination of the time-dependent offshore sediment transport S_y in the D-profile of the form:

$$S_y = r(R_\infty - R_t) \qquad ....(7)$$

where S_y = time-dependent offshore sediment transport in the D-profile
R_t = a time-dependent D-profile characteristic, which will be defined later
R_∞ = the equilibrium value of R_t, i.e. $R_t \xrightarrow[\infty]{t} R_\infty$
r = o constont for o specific set of boundary conditions.

A study of various possible forms of the function R_t reveoled that if R_t is chosen as a schematic length (L_2-L_1) (see Figure 1 for an explanation of (L_2-L_1)), a reasonobly good correspondence is obtained with the available test results. Thus on equation of the following form results:

$$S_y = s_y\,(W - (L_2 - L_1)_t) \qquad ....(8)$$

where $(L_2 - L_1)_t$ = value of $(L_2 - L_1)$ at time t.
W = equilibrium value of $(L_2 - L_1)$
s_y = a constant for a specific set of boundary conditions.

If s_y and W are known, the offshore transport S_y con be calculated for any location in the D-profile by moking an oppropriate choice of the onshore- and offshore profile thicknesses δ_1 and δ_2 respectively (see Figure 1).

4 Evaluation of the data

In order to enable the prediction of s_y and W in terms of the wave conditions and bed material characteristics, all available appropriate small- and full-scale tests were elaborated. The criteria handled for the choice of the tests to be used for the evaluation of the schematization, are the following: (1) frequent soundings of the bed must be available, to allow a good extrapolation of the time-dependent data to the equilibrium situation, and (2) no secondary effects must have occurred. Secondary effects can either originate from an imperfect motion of the wave board, or from the shoaling and breaking of waves over bars in the nearshore D-profile. Secondary effects of the first type are clearly restricted to model tests, the second type of secondary effect can occur both in the model and the prototype. Consequently tests in which secondary effects of the first type occurred were not evaluated, while the tests with secondary effects of the second kind were evaluated. From the remaining tests results of the form shown in Figure 5 were obtained. The curve of the equilibrium length W against the dimensionless position in the D-profile (δ_1/δ) determines fully the equilibrium D-profile, while a combination of the two curves enables the calculation of the offshore transport at any time in a non-equilibrium profile.

5 The equilibrium length W

The W-curve can be fully determined if the value of W at for instance the water line (W_r) is known, as well as the ratio W/W_r in the rest of the profile.

In order to enable the calculation of the value of W_r as a function of the boundary conditions, a representative slope m_r was defined:

$$m_r = \frac{\delta}{2W_r} \qquad \text{.......(9)}$$

where m_r = schematized equilibrium slope of the D-profile at the water line.

Earlier studies regarding the criteria which will determine the transition between step and bar profiles, (see Nayak[7]), revealed that the deepwater wave steepness H_o/λ_o, the absolute value of the wave weight H_o and the sediment particle diameter D_{50} are of importance. In a study to determine the transition between erosion and accretion in the area above the water line [8], it was found that the average slope m_a at the water line was also of influence. In the present study the schematic equilibrium slope m_r was used instead of the average actual slope. When this approach was applied to the available model and prototype data in the same manner as described in [8], good results were obtained, as can be seen in Figure 6, which yields a relationship of the form:

$$m_r \frac{H_o}{\lambda_o} = 1.51 * 10^3 \left[H_o^{\ 0.132} D_{50}^{\ -0.447} \left(\frac{H_o}{\lambda_o}\right)^{-0.717} \right]^{-2.38} + 0.11 * 10^{-3} \quad ....(10)$$

Equation (10) defines the value of W_r for a specific set of boundary conditions.

The variation in the ratio W/W_r over the D-profile determines the dimensionless form of the D-profile. Wiegel [10] classified beaches into three groups, viz. protected, moderately protected and exposed beaches. For each of these three types of beaches he gives a relationship between the beach slope in the area between the limit of wave run-up and the low-water line and the median particle diameter D_{50}. An increase in particle diameter leads to an increase in beach slope. Eagleson et al [2] studied the forces on a discrete spherical bed load particle outside the breaker zone. They predicted the slope of the bed in this area as a function of the boundary conditions. For bigger particle diameters the slope decreases. The above-mentioned two results indicate that the curvature of profiles with coarser bed material is bigger than with finer bed material. This conclusion is confirmed by the elaborated results (see [9]). An equation for W/Wr of the following form (see Figure 7) was found:

$$\frac{W}{W_r} = 0.7\,\Delta_r + 1 + 3.97 * 10^7\, b\, D_{50}^{\ 2}\, \Delta_r^{\ 1.36 * 10^4 D_{50}} \quad ....(11)$$

where $\Delta_r = \dfrac{h_m - \delta_2}{\delta}$ = dimensionless position in the D-profile, measured positively downwards from the still-water level.

$b = \begin{cases} 1 & \text{for } \Delta_r > 0, \text{ i.e. below the still-water level} \\ 0 & \text{for } \Delta_r \leqslant 0, \text{ i.e. above the still-water level.} \end{cases}$

A correlation of equation (11) to all available small-scale three-dimensional model tests and prototype cases revealed that this equation can also be applied to these conditions, without making a significant error.

6 The coastal constant s_y (two-dimensional case)

The s_y-curve can be fully determined if, (1) the maximum value s_{ym} of s_y, (2) the location of s_{ym} and (3) the distribution of s_y/s_{ym} across the D-profile is known.

A study of the available literature on the formation of step and bar profiles, as summarized by Nayak [7], led to the conclusion that s_{ym} will be determined by the following relationship:

$$s_{ym} = f\,(H_o/\lambda_o,\ H_o\,T,\ D_{50},\ H_o/h_m) \qquad \text{.......(12)}$$

where H_o/h_m = a measure of the type of breaking wave.

A correlation of this formula to the available small- and full-scale data led to the following equation (see Figure 8):

$$\ln\left(\frac{s_{ym}T}{D_{50}}\right) = 10.7 - 28.9\left[H_a^{1.68}\left(\frac{H_o}{\lambda_a}\right)^{-0.9} D_{50}^{-1.29}\left(\frac{H_a}{h_m}\right)^{2.66}\right]^{-0.079} \qquad \text{...(13)}$$

A study of the available data led to the conclusion that the position of the maximum value of s_y will be a function of the ratio H_o/h_m and the absolute value of the wave height, (see Figure 9), viz.:

$$\Delta_{2m} = 0.8 - 1.1\,H_a^{-0.55}\left(\frac{H_a}{h_m}\right)^{2.69} \qquad \text{.......(14)}$$

When the characteristics of the backshore erosion, transition slope growth, the distribution across the D-profile of W, the location and magnitude of s_{ym} are all known, it can be shown (see [9]) that it is possible to calculate mathematically the distribution of s_y across the D-profile. As this is, however, a tedious procedure involving the solution of seven non-linear equations, an approximate distribution of s_y/s_{ym} was determined from the available test results (see Figure 10), viz.:

In the area landwards of the location of s_{ym}:

$$s_y/s_{ym} = \frac{0.93}{1 + 1.01\,X^{2.11}} + 0.07 \qquad \text{.......(15)}$$

In the area seawards of the location of s_{ym} :

$$s_y / s_{y_m} = \frac{0.99}{1 + 1.14\, X^{2.11}} + 0.01 \qquad \ldots\ldots.(16)$$

In both coses

$$X = \Delta_m \left(\frac{H_o}{\lambda_o} \right)^{-1} \left(\frac{H_o}{h_m} \right)^2 \qquad \ldots\ldots.(17)$$

where Δ_m = obsolute value of the dimensionless position in the D-profile, meosured relative to the locotion of s_{y_m}

$$= \left| \frac{\delta_2 - \delta_{2m}}{\delta} \right|$$

δ_{2m} = volue of δ_2 where $s_y = s_{ym}$.

As both s_y ond W are now known, it is possible to determine both the equilibrium profile ond the offshore sediment transport in the two-dimensionol cose.

7 The coostol constant s_y (three-dimensional cose)

Due to the superposition of a longshore current to the wave field, the momentary resultant current velocities at the bed, as well as the resultant bed sheor in the three-dimensional case, will be higher than in the two-dimensional case. As has been stated eorlier, the values of W for the two- and three-dimensional cases do not differ significantly from each other. As the sediment transport is a function of the bed shear, it seems reolistic to assume that the offshore transport rate of sediment in the three-dimensional cose will be higher than in the two-dimensional case. This implies that s_y will also be higher than for the two-dimensional case. The mean increase in the bed sheor due to a combined current and wave action can be found by numerical integration, viz.:

$$\frac{\overline{\tau_{wc}}}{\tau_w} = 1 + (1.91 - 1.32 \sin \phi_b) \left(\frac{v}{\xi_J u_o} \right)^{(1.24 - 0.08 \sin \phi_b)} \qquad \ldots\ldots.(18)$$

where $\xi_J = C_h \sqrt{\frac{f_w}{2g}}$

C_h = Chézy-coefficient

f_w = wave friction factor, according to Jonsson [6] .

v = average longshore current velocity at a certoin water depth

u_o = orbital velocity at the bed

ϕ_b = angle of wave incidence at breaking

τ_{wc} = bed shear due to combined current ond wove action

τ_w = bed shear due to current action only.

The increase in the coostal constant s_{ym} can be correlated to the increose in bed sheor, viz.:

$$\frac{s_{ym3D}}{s_{ym2D}} = \left(\frac{\overline{\tau_{wc}}}{\tau_w} \right)^{4.5} \qquad \ldots\ldots.(19)$$

where s_{ym2D} ond s_{ym3D} are the two- and three-dimensionol volues respectively of s_{ym}.

A cambination of equations (13), (18) and (19) will yield the value of s_{ym} in the three-dimensionol case. The location af this volue is still given by equotion (14). The distribution of s_y/s_{ym} should be calculoted with the aid of the mothematical procedure involving 7 non-linear equotions, which hos olready been mentioned in section 6, and which is derived elaborately in [9].

8 Applicotion of the theory

The method described in this poper can be used to compute time-dependent and equilibrium profiles, as well os the carresponding offshare sediment losses. In Figure II o comparison is shown between o final profile, given by Eogleson et al [3], and a theoreticol equilibrium prafile, colculoted with the aid af equatians (10) ond (11). The correspondence is rather good. In Figure 12 a comporison is given between measured and theoretically computed offshare sediment losses, for o storm period in the Netherlonds in February, 1953. The exoct longshore current velocities ore nat known, hawever, os can be seen, the order of magnitude of the computed lasses correspands well with the measured losses. The method can olso be used to campute offshore sediment losses after beach replenishment.

9 Restrictians and recommendotions

When applying the theory, it should be kept in mind that the lower limit of the D-profile hos been determined by using the assumptian thot $D_{50} \leqslant 0.5$ mm. This places o restriction on the maximum porticle size for which the methad can still be applied. All tests used for the elobarotion in the present study were perfarmed with regular wave attock. Under prato-type conditions, where the woves are randam, the wave spectrum will determine which representotive wave height should be used in the opplicotion. This ospect of the problem shauld be studied in more detoil. A test programme should be designed to ossist in the extension of the theory ta include onshore sediment movement.

10 Conclusions

The principal conclusions of the investigation described in this paper may be summarized as follows:

(1) The upper limit of the actual developing profile (called D-profile in this paper) is related to the maximum wave run-up and is of the form given in equation (4).
(2) The lower limit of the D-profile is related to the beginning of movement of bed material under wave action and is of the form given in equation (6).
(3) The offshore transport at any location in the D-profile at any time t is proportional to the difference between the equilibrium profile form and the profile form at time t, according to equation (8).
(4) The sediment transport at the upper and lower limits of the D-profile are not necessarily negligible; these transport follow the same time-dependent variation as given by equation (8).
(5) The form of the dimensionless equilibrium D-profile is determined by the particle diameter according to equation (11).
(6) The horizontal scale of the equilibrium D-profile is determined by the absolute value of the deepwater wave height, the deepwater wave steepness and the particle diameter, according to equation (10).
(7) The equilibrium beach slope at the upper limit of the D-profile increases with increasing particle diameter, while the equilibrium slope at the lower limit of the D-profile decreases with increasing particle diameter.
(8) The equilibrium D-profile under three-dimensional conditions is as a first approximation equal to that under corresponding two-dimensional conditions.
(9) The rate of offshore transport under three-dimensional conditions is higher than under corresponding two-dimensional conditions, due to the increase in the average bed shear (equation 19)).

REFERENCES

1 BONNEFILLE, R. and PERNECKER, L.
"Le début d'entrainement des sédiments sous l'action de la houle";
Bulletin du Centre de Recherches et d'Essais de Chatou, No. 15, Mars, 1966.

2 EAGLESON, P.S., DEAN, R.G., and PERALTA, L.A.
The mechanics of the motion of discrete spherical and bottom sediment particles due to shoaling waves;
Beach Erosion Board, Technical Memorandum No. 104, Washington, 1958.

3 EAGLESON, P.S., GLENNE, B. and DRACUP, J.A.
Equilibrium characteristics af sand beaches;
Praceedings ASCE, J. Hydraulics Divisian, Paper Na. 3387, pp. 35-57, Valume 89, January, 1963.

4 GODDET, J.
"Etude du début d'entrainement des matérieux mabiles sous l'actian de la haule";
La Hauille Blanche, Na. 2, pp 122-135, Mars-Avril, 1960.

5 HUNT, I.A.
Design af seawalls and breakwaters;
Praceedings, ASCE, Jaurnal of the Waterways and Harbaurs Divisian, 85, Na. WW3, paper 2172, pp. 123-152, September, 1959.

6 JONSSON, I.G.
Measurements in the turbulent wave baundary layer;
Praceedings, 10th I.A.H.R. Congress, Landan, Volume I, Paper 1-12, pp. 85-92, 1963.

7 NAYAK, I.V.
Equilibrium prafiles af madel beaches;
Ph.D. thesis, University af Califarnia, Califarnia, 1970.

8 SWART, D.H.
The effect af distartian an caastal prafiles (in Afrikaans);
M.Eng.thesis, University af Stellenbasch, Sauth Africa, 176 pp., March, 1971.

9 SWART, D.H.
Offshare transpart and equilibrium prafiles;
Publicatian na. 131, Delft Hydraulics Labaratary, 244 pp., 1974.

10 WIEGEL, R.L.
Oceanagraphical Engineering;
Englewaad Cliffs, New Jersey, Prentice Hall, 532 pp., 1964.

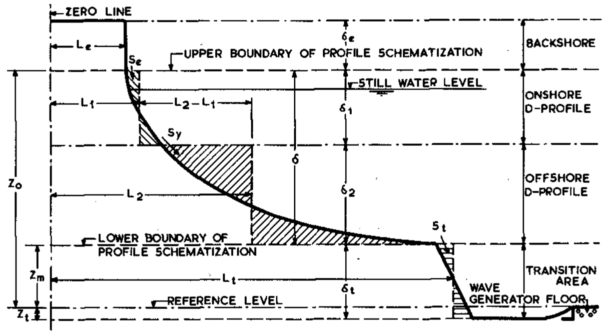

Figure 1: Schematization of beach profile

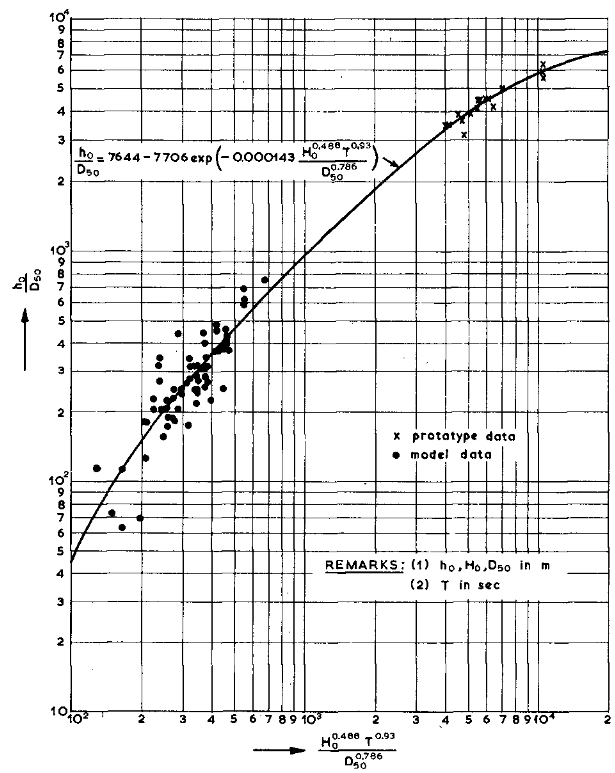

Figure 2: Upper limit of D-profile

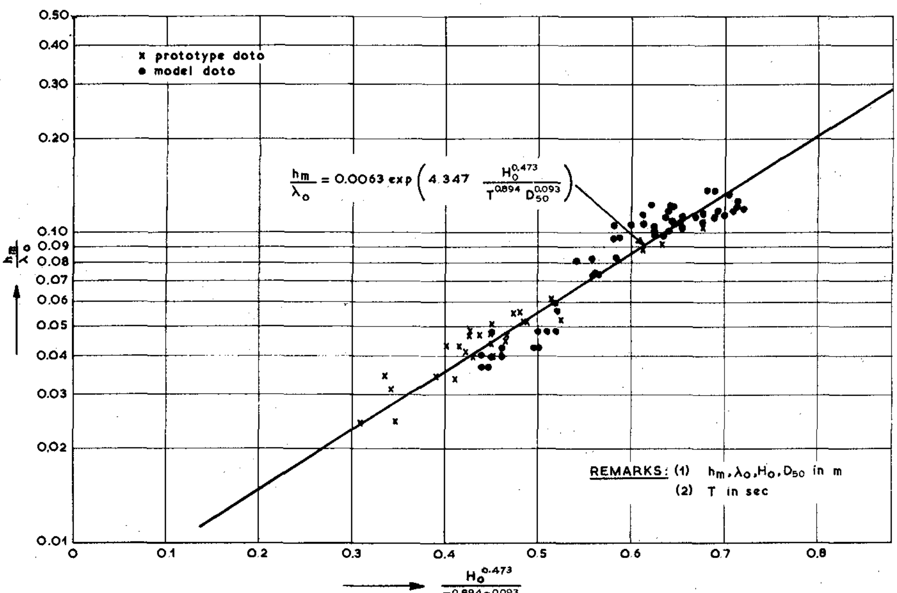

Figure 3: Lower limit of D-profile

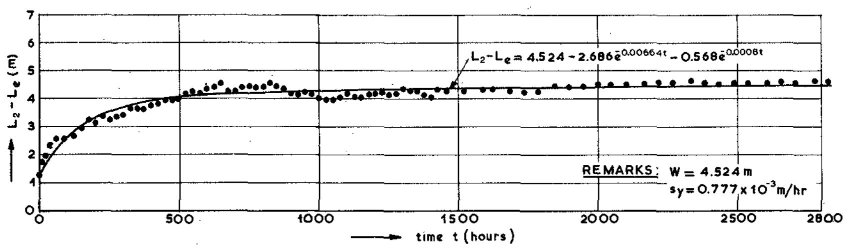

Figure 4: Time-variation of $(L_2 - L_e)$

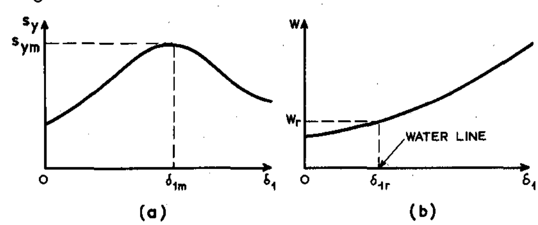

Figure 5: Form of results

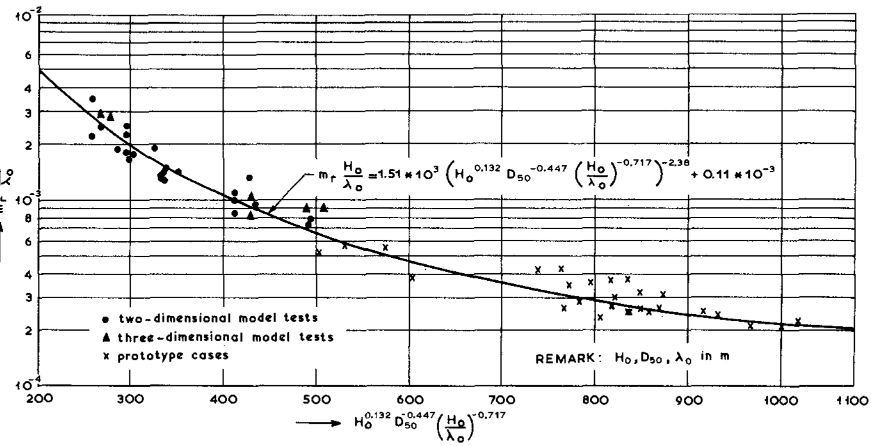

Figure 6: Horizontal scale of the equilibrium D-profile

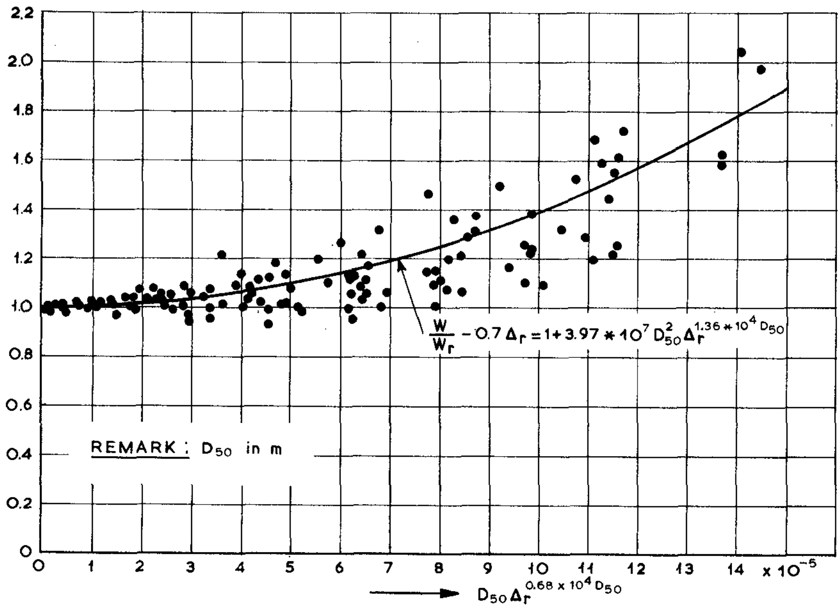

Figure 7: General relationship for W/W_r (two-dimensional cases)

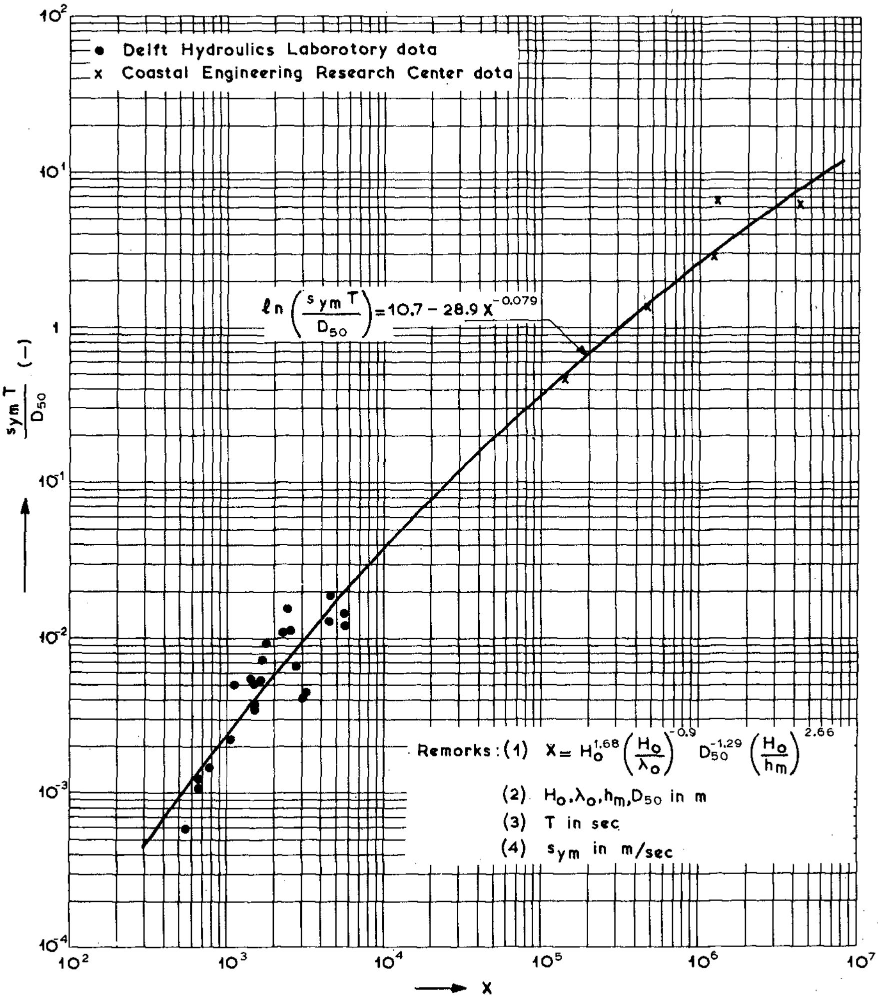

Figure 8: Magnitude of s_{ym}

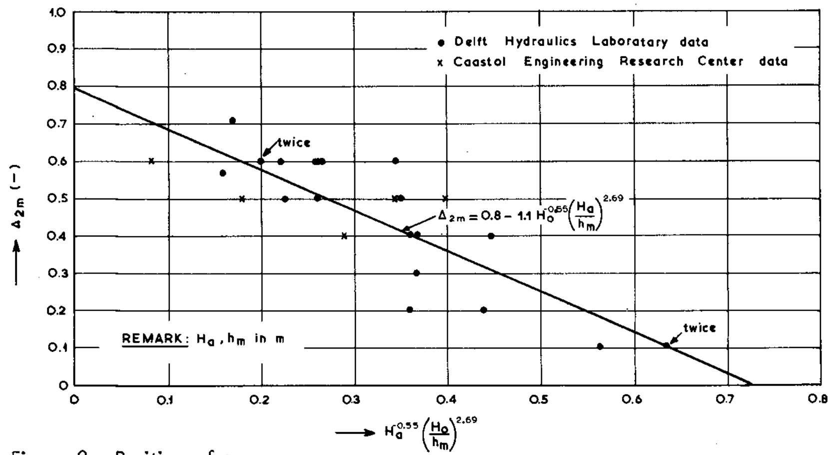

Figure 9: Position of s_{ym}

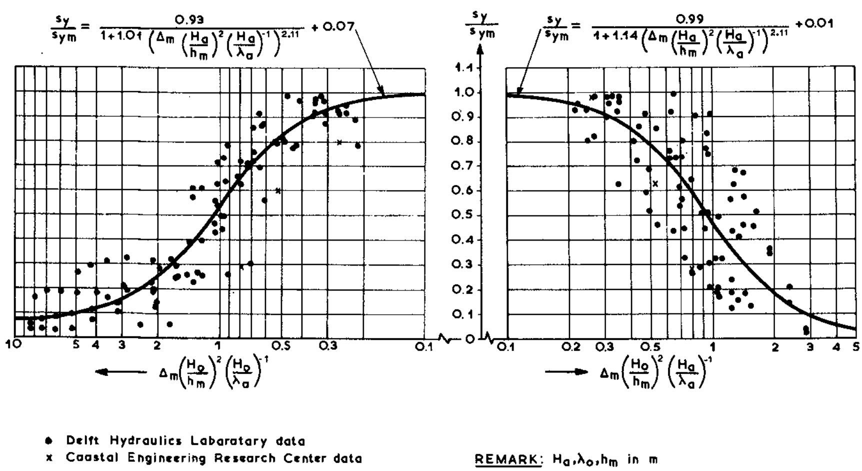

Figure 10: Distribution of s_y/s_{ym}

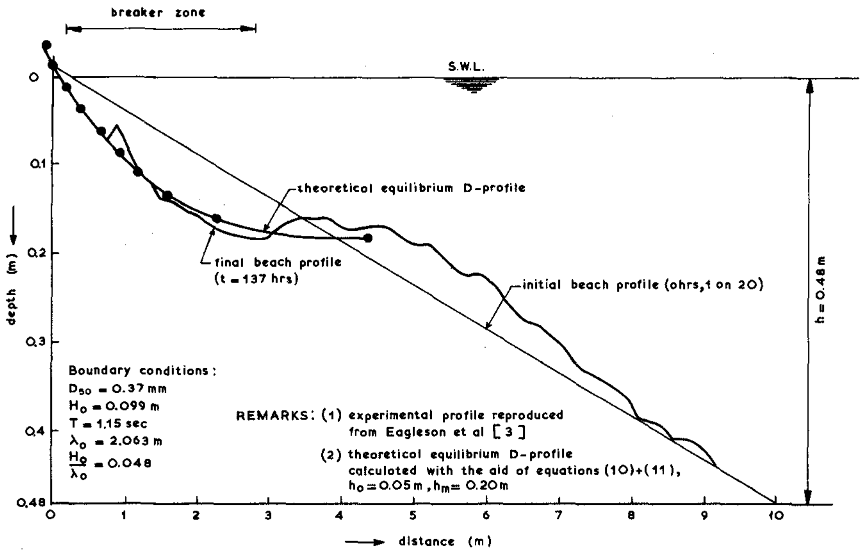

Figure 11: Comparison of theoretical and experimental equilibrium profiles

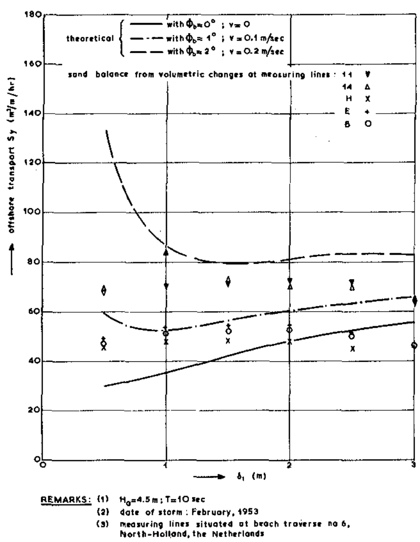

Figure 12:

Comparison of theoretical and measured transport rates in prototype